

Pharmacokinetics of quercetin-loaded nanodroplets with ultrasound activation and their use for bioimaging

Li-Wen Chang¹
Mei-Ling Hou¹
Shuo-Hui Hung²
Lie-Chwen Lin³
Tung-Hu Tsai^{1,4-6}

¹Institute of Traditional Medicine, School of Medicine, National Yang-Ming University, ²Department of Surgery, ³National Research Institute of Chinese Medicine, Ministry of Health and Welfare, Taipei, ⁴Department of Education and Research, Taipei City Hospital, ⁵School of Pharmacy, College of Pharmacy, Kaohsiung Medical University, Kaohsiung, ⁶Graduate Institute of Acupuncture Science, China Medical University, Taichung, Taiwan

Abstract: Bubble formulations have both diagnostic and therapeutic applications. However, research on nanobubbles/nanodroplets remains in the initial stages. In this study, a nanodroplet formulation was prepared and loaded with a novel class of chemotherapeutic drug, ie, quercetin, to observe its pharmacokinetic properties and ultrasonic bioimaging of specific sites, namely the abdominal vein and bladder. Four parallel groups were designed to investigate the effects of ultrasound and nanodroplets on the pharmacokinetics of quercetin. These groups were quercetin alone, quercetin triggered with ultrasound, quercetin-encapsulated in nanodroplets, and quercetin encapsulated in nanodroplets triggered with ultrasound. Spherical vesicles with a mean diameter of 280 nm were formed, and quercetin was completely encapsulated within. In vivo ultrasonic imaging confirmed that the nanodroplets could be treated by ultrasound. The results indicate that the initial 5-minute serum concentration, area under the concentration–time curve, elimination half-life, and clearance of quercetin were significantly enhanced by nanodroplets with or without ultrasound.

Keywords: nanodroplets, quercetin, ultrasonic pharmacokinetics, ultrasonic imaging, ultrasound

Introduction

The development of nanomedicine arose from a combination of nanotechnology and medicine, and due to the special properties of nanosized particles, nanomedicine provides potential encapsulation systems for medical agents used in both diagnostic and therapeutic applications.^{1,2} In the field of therapeutic applications, nanomedicines offer advantages over conventional medicines, including improvement of poor drug solubility, increased bioavailability,^{3,4} and targeted delivery of chemotherapeutic drugs.^{5,6} Application of nanotechnology to imaging methodologies is paving the way for diagnostic medicine. Nanoparticles have been designed and used as detectors for diagnostic application in clinical and basic medical research, including magnetic resonance imaging,⁷ positron emission tomography,⁸ IVIS® spectrum imaging,⁹ and ultrasonic imaging.^{10,11} Ultrasonic imaging, a noninvasive and real-time procedure, is often used. Compared with other imaging techniques, ultrasound systems are cost-effective, portable, easy to use, and safe for both clinical staff and patients over repeated use due to lack of ionizing radiation.¹²

Bubble formulations represent a new class of encapsulation systems with both diagnostic and therapeutic applications.¹¹ They can transport drugs or genes to a specific location, at which point ultrasound is applied, causing the formulations to burst and leading to site-specific delivery of bioactive materials.¹³ In addition to targeted drug

Correspondence: Tung-Hu Tsai
Institute of Traditional Medicine, School of Medicine, National Yang-Ming University, 155, Section 2, Li-Nong Street, Taipei 112, Taiwan
Tel +886 2 2826 7115
Fax +886 2 2822 5044
Email thtsai@ym.edu.tw

delivery, bubble formulations have also received attention as ultrasonic imaging agents. Micron-scale (μm) bubbles (microbubbles) can become trapped in the blood pool after intravenous injection. The reported use of microbubbles has largely been limited to research involving cardiovascular diseases, including inflammation, arteriosclerosis, and thrombus formation.^{14,15} In addition, microbubbles are often restricted in their utility for tissue-targeted imaging due to their large diameters.^{15,16} Therefore, nanoscale bubbles (nanobubbles) and nanodroplets have been developed and studied as contrast agents and drug carriers for diagnostic and therapeutic application due to their particle size.^{11,15,17}

A large number of polymeric nanoparticles have been evaluated when applied in basic and clinical medical studies. Many of these particles were able to alter the distribution profiles of encapsulated drugs.^{1,18} However, previous literature reports have indicated that these nanobubbles/nanodroplets are still in the early stages of development,^{19,20} whether in ultrasonic imaging or therapeutic applications.

Generally, the shells of nanobubbles are composed of nontoxic biodegradable materials (such as albumin or lipids), and encapsulated with poorly soluble and nonreactive gases (such as inert air or perfluorocarbon).²¹ Perfluoropentane (C_5F_{12}) is a liquid at room temperature, boils at 28.5°C , and is generally used to generate nanobubbles as gas. When these shells were filled with perfluoropentane to form nanodroplets,²² they can be activated by heat or other energy to form nanobubbles.²³

To our knowledge, there are no studies that have investigated the pharmacokinetics of drug-loaded nanobubbles/nanodroplets with ultrasound treatment. Additionally, the applications of nanobubble/nanodroplet ultrasound imaging are currently limited to observing tumor tissue.^{15,24} In this study, we designed perfluoropentane nanodroplets to investigate ultrasound-induced pharmacokinetics and development of novel diagnostic applications to improve our understanding of and ability to accurately predict the clinical applications and efficacy of echogenic bubbles.

Quercetin is a plant-derived bioflavonoid that is found in naturally occurring products. Pharmacological reports have demonstrated that quercetin has pronounced pharmaceutical effects, including anti-inflammatory, antioxidant, and antiviral activity.²⁵ In addition, quercetin is included in a novel class of chemotherapeutic drugs for the treatment of various cancers²⁶ and can also be combined with ultrasonic pretreatment to increase the concentration of quercetin to inhibit the growth of the prostate and skin cancer cell lines.²⁷ However, quercetin has low aqueous solubility, poor absorption, and rapid

metabolism (bioavailability approximately 1%–5%),²⁸ all of which can generate in vivo results that differ from the powerful in vitro efficacy of quercetin. Thus, encapsulation of quercetin in nanodroplets may improve its pharmacokinetic profile, and with the use of ultrasound-triggered rupturing, enable effective drug delivery to provide anticarcinogenic effects.^{29,30}

The current study aimed to: design lipid-coated nanodroplets containing quercetin; evaluate the functions of the formulations in terms of their physicochemical characteristics after in vitro release of quercetin; assess their potential diagnostic applications by in vivo ultrasonic imaging of topical tissue (bladder) and the vascular system; and investigate the pharmacokinetic profile of quercetin loaded into nanodroplets and of ultrasound-triggered quercetin-loaded nanodroplets.

An improved understanding of the effect of combining quercetin-loaded nanodroplets with ultrasonic treatments on bioimaging and pharmacokinetics may help to better predict the clinical applications of nanodroplets and lead to more effective design preparation.

Materials and methods

Materials and experimental animals

Perfluoropentane (96%, boiling point 28.5°C) was purchased from Strem Chemicals (Newburyport, MA, USA). Cholesterol, coconut oil, quercetin, heparin, α -chloralose urethane, and polyethylene glycol (PEG) 400 were obtained from Sigma-Aldrich Co. (St Louis, MO, USA). Hydrogenated soybean phosphatidylcholine (Phospholipon[®] 80H) was supplied by American Lecithin Company (Oxford, CT, USA). Distearoyl phosphatidyl ethanolamine-PEG with a mean molecular weight of 5,000 (DSPE-PEG 5000) was obtained from Nippon Oil & Fats Co., Ltd (Tokyo, Japan). The cellulose membrane (Cellu-Sep[®] T2, molecular weight cut-off 6,000–8,000 Da) was obtained from Membrane Filtration Products Inc. (Seguin, TX, USA). Ethanol, chloroform, ethyl acetate, methanol, and acetonitrile were purchased from EMD Millipore (Billerica, MA, USA). Triply deionized water from EMD Millipore) was used in the preparation of all aqueous solutions.

Adult male Sprague-Dawley rats (200 ± 30 g body weight) were obtained from the National Yang-Ming University Animal Center, Taipei, Taiwan. The animals were specifically pathogen-free and had free access to food (Laboratory Rodent Diet 5001, PMI Nutrition International LLC, St Louis, MO, USA) and water. All experimental protocols involving animals were performed and approved by the Institutional Animal Care and Use Committee (1010613) of National Yang-Ming University.

HPLC analysis of quercetin

The high-performance liquid chromatography (HPLC) system was composed of a chromatographic pump (LC-20AT, Shimadzu, Kyoto, Japan), an autosampler (SIL-20AT, Shimadzu), a diode array detector (SPD-M20A, Shimadzu), and a degasser (DGU-20A5). A reversed-phase C18 column (250×4.6 mm, particle size 4 μm, Synergi Fusion RP 80, Phenomenex, Torrance, CA, USA) was used. The mobile phases consisted of acetonitrile 10 mM KH₂PO₄ (47:53, v/v) at pH 3.0, and the flow rate was 1 mL per minute. The ultraviolet wavelength was set to 370 nm and the sample injection volume was 20 μL. The limits of detection and quantification were defined as a signal-to-noise ratio of 3 and the lowest concentration from the linear regression, respectively.

Preparation of the nanodroplet-encapsulated quercetin formulation

Soybean phosphatidylcholine (4.0%, w/v of the final product), cholesterol (1%, w/v), and DSPE-PEG 5000 (1%, w/v) were dispersed in 5 mL of a chloroform-methanol (2:1) solution. The organic solvent was evaporated in a rotary evaporator at 50°C, and the solvent traces were removed by maintaining the lipid film under a vacuum overnight. The film was hydrated with triply deionized water containing quercetin (solubility approximately 60 mg/L) using a probe-type sonicator (VCX600, Sonics and Materials, Newtown, CT, USA) at 35 W for 10 minutes at 60°C. Coconut oil 3.0% was then added to the mixture, followed by high-shear homogenization (Pro250, Pro Scientific, Monroe, CT, USA) for 5 minutes. The semi-finished product was cooled to 0°C. Finally, perfluoropentane (10%, w/v) was incorporated into the system, followed by homogenization (for 5 minutes at 0°C) and sonication (35 W for 5 minutes at 0°C). The total volume of the resulting product was set at 5 mL. After the formulations were prepared, they were left to stand for 1 day at 0°C degassed.

Determination of particle size and zeta potential

The mean particle size and polydispersity index of the formulations were measured by dynamic light scattering (90 Plus, Brookhaven Instruments Corporation, Holtsville, NY, USA). The zeta potential of the formulations was determined using a zeta potential analyzer (90 Plus, Brookhaven Instruments Corporation). The dispersion of the prepared formulations was diluted tenfold with triply deionized water for measurement of both size and surface charge. Particle characterizations were repeated three times per sample for three independent batches.

Encapsulation of quercetin in nanodroplets

Entrapment capacity was used to determine the amount of drug in the nanodroplet-encapsulated quercetin (NQ) formulation. The NQ formulations were centrifuged at 48,000× g at 4°C for 30 minutes in an Optima Max[®] ultracentrifuge (Beckman Coulter, Brea, CA, USA) to separate the incorporated drug from the free form. The samples were collected from the supernatant at top of the tube. The amount of quercetin in the formulation was analyzed using the HPLC system. The entrapment capacity of NQ was calculated as follows: $([\text{total amount of drug} - \text{amount of drug detected only in the supernatant}]/\text{total amount of drug}) \times 100$.³¹ Three formulations were tested, and the data are expressed as the mean ± standard deviation (n=3).

Morphological observations by TEM

The characteristic microstructure of NQ was assessed by transmission electron microscopy (TEM) as follows. First, a drop of a formulation (the formulation was diluted tenfold by triply deionized water) was applied to a 400-mesh carbon film-covered copper grid to form a thin film specimen, which was stained with 2% phosphotungstic acid (40 seconds). After the stained samples were allowed to dry in air, TEM samples were obtained. The samples were prepared at room temperature (about 22°C–24°C). The sample was then examined and photographed by TEM (JEM-1400EXII, JEOL, Tokyo, Japan).

In vitro drug release study

The drug release profile for the NQ formulation was measured using a Franz diffusion cell. A cellulose membrane (molecular weight cut-off 6,000–8,000 Da) was mounted between the donor and acceptor compartments, acting as a barrier in the experiments to examine drug release from the NQ. The donor medium consisted of 0.5 mL of vehicle containing the drug and a 0.5 mL sample of rat plasma and was added (or not added) to the donor compartment. The receptor medium consisted of 5.5 mL of ethanol with pH 7.4 buffer (3:7 ratio) to maintain physiological conditions. The practical diffusion area between the cells was 0.785 cm². The stirring rate and temperature of the receptor were maintained at 600 rpm and 37°C, respectively. At each time point, 0.3 mL aliquots of the receptor medium were removed and immediately replaced by equal volumes of blank buffer. The concentration of quercetin released was determined using the HPLC system. In the study exploring the release of drug from NQ with or without ultrasound, the donor phase was exposed to ultrasound using a 1 MHz probe (Rich-Mar

Sonitron 2000, Inola, OK, USA) with a 2.0 W/cm² intensity and a 20% duty cycle.

In vivo ultrasonic imaging

To evaluate in vivo ultrasonic imaging of nanodroplets, the femoral vein was catheterized with polyethylene tubing for intravenous administration under anesthesia (urethane 1.0 g/kg and α -chloralose 0.1 g/kg). Ultrasonic scanning was performed by means of an Acuson S2000TM ultrasound system (Siemens, Washington, DC, USA) with a 9 MHz linear array probe. An initial baseline B-mode survey and a color/power Doppler analysis were performed. Ultrasound scan parameters, such as focal zone, persistence, linear gray-scale map, time-gain compensation curve, and focal settings, were fixed throughout the experiment. Next, the ultrasound device was set to cadence contrast pulse sequencing mode with a transmission frequency of 7 MHz and a mechanical index of 0.18 to avoid destruction of the formulation. About 1 minute after injection, the mechanical indices (MI) was manually adjusted and fixed to 1.0 for destruction of the formulation. Each examination lasted approximately 6 minutes after the bolus injection.

Surgical procedures

The rats were initially anesthetized using a mixture of urethane 1.0 g/kg and α -chloralose 0.1 g/kg. A polyethylene tube was implanted into the right external jugular vein and femoral vein to collect blood and for drug administration, respectively. Subsequently, for the groups receiving ultrasound treatment, the hilum of the liver was gently exposed through a midline incision so that the hepatic portal vein could be accessed. Three minutes after drug administration then treated with ultrasound for 1 minute using a 1 MHz probe with a 2.0 W/cm² intensity and a 20% duty cycle.

Drug administration and sampling

Quercetin (dissolved in PEG 400 with 20% ethanol) or an equal quercetin dose in NQ (3 mg/kg) was intravenously injected via the femoral vein. A 500 μ L aliquot of the blood sample was withdrawn from the jugular vein into a heparin-rinsed vial using a fraction collector set to a programmed schedule at 5, 10, 20, 30, 45, 60, 90, and 120 minutes.

Sample preparation

The blood samples were centrifuged at 16,000 \times g for 10 minutes at 4°C for plasma preparation. The supernatant was collected for plasma samples and preserved at -20°C before further sample analysis. A 50 μ L aliquot of the plasma sample, 5 μ L of internal standard apigenin (10 μ g/mL), and 1,000 μ L

of ethyl acetate were added, and the mixture was vortexed for 30 seconds. The mixture was centrifuged at 16,000 \times g for 10 minutes at 4°C. The supernatant (950 μ L) was transferred to tubes and dried under vacuum at room temperature. Finally, the samples were reconstituted in 50 μ L of 50% acetonitrile, and 20 μ L of the mixture was injected into the HPLC system.

Statistical analysis

All pharmacokinetic analyses were carried out using WinNonlin Standard Edition version 1.1 (Scientific Consulting Inc, Apex, NC, USA). A noncompartmental model was utilized for the data fitting and parameter estimation. The pharmacokinetic results are represented as the mean \pm standard error of the mean. Statistical significance was determined using one-way analysis of variance, followed by a Schiff post-test using Statistical Package for the Social Sciences version 10 software (SPSS Inc., Chicago, IL, USA), with $P < 0.05$ accepted as the minimal level of significance.

Results

Physicochemical characteristics of nanodroplets and NQ

These formulations were prepared using the conventional thin film hydration technique, and the lipid film was prepared by modifying previous experimental methods, including modifying the evaporation temperature and vacuum time.^{20,32-34} Therefore, the organic solvents could be completely removed under these conditions, and even if there were slight solvent residues, they did not affect the subsequent experiments.

Because perfluorocarbon-loaded nanodroplets are satisfactorily stable when circulating in the vasculature as blood pool agents, they act as carriers of these agents until the site of interest is reached.¹³ In this study, the formulation system containing perfluoropentane (with a boiling point of 28.5°C) was designed with soybean phosphatidylcholine, cholesterol, and DSPE-PEG 5000. The use of DSPE-PEG 5000 in nanodroplets can aid in increasing the circulation time in vivo and for sustained drug release.³⁵ Coconut oil is extracted from coconut (kernel or meat), and was used as the oil phase due to its superiority in enhancing flavonoid solubility compared with other oils.^{36,37} Perfluoropentane is a nonpolar and hydrophobic substance, which can disperse in aqueous solution by surfactants.³⁸ Cholesterol is an amphipathic compound containing both a water-soluble region and a fat-soluble region, regulating the lipid structure to improve the stability of formulations.³⁹ Therefore, the core of the formulation was loaded with perfluoropentane, which was surrounded

by coconut oil. Soybean phosphatidylcholine, DSPE-PEG 5000, and cholesterol, which functioned as emulsifiers, were located at the oil/water interface as a phospholipid membrane surrounding the quercetin-containing core.

To evaluate the physicochemical properties of the formulations, the particle size and zeta potential were examined. Table 1 summarizes the physicochemical characteristics of the nanodroplets and the NQ formulation. Dynamic light scattering indicated that the size of the nanodroplets and the NQ formulation was approximately 280 nm with a polydispersity index <0.35 , suggesting that the particle formulations were quite homogeneous. The zeta potentials of the nanodroplets and NQ were -42.18 and -34.66 mV, respectively. To calculate the loading of quercetin in the nanocomplex, nanoparticle counting instruments (such as Q-Nano) may be used to estimate the number of NQ particles. However, this method provides only a rough estimate due to the potential for errors associated with sample preparation (filtering of the sample may cause errors in number of particles counted). Therefore, we used encapsulation efficiency as an acceptable alternative. The entrapment capacity of NQ was calculated as follows: $([\text{total amount of drug} - \text{amount of drug detected only in the supernatant}]/\text{total amount of drug}) \times 100$.³¹ The encapsulation efficiency of NQ was 99% (about 2.97×10^{19} molecules of quercetin were encapsulated).

Stability of NQ formulation

Loss of gas is the main reason for destruction of bubble formulations.⁴⁰ To assess the stability of NQ in the body and during storage in a freezer, the NQ formulation was evaluated using a 37°C oven and a 4°C freezer. As shown in Figure 1, NQ evaporated rapidly within 10 hours at 37°C and completely evaporated after 24 hours; however, the weight of NQ did not change significantly over 0–24 hours at 4°C . The size and zeta potential of the NQ formulation was also measured at 4°C after 24 hours, and the results indicated no significant differences from values recorded at 0 hours.

TEM of NQ formulation

TEM with a multifunctional nanosensor was used to image and quantify the mechanical properties of the NQ formulation.⁴¹

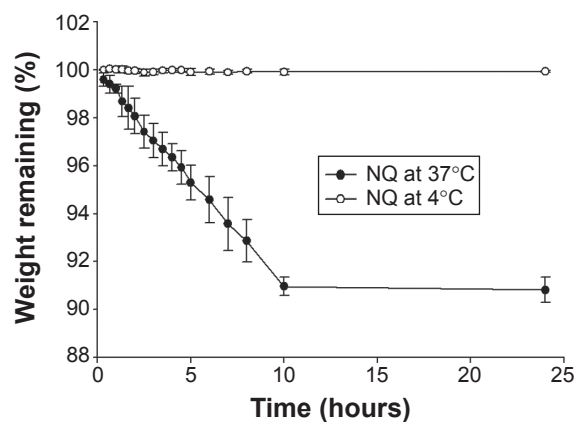


Figure 1 Percentage weight remaining in the NQ formulation as a function of time in the stability experiment in a 37°C oven and 4°C freezer. Each value represents the mean \pm standard deviation ($n=4$).

Abbreviation: NQ, nanodroplet-encapsulated quercetin.

Figure 2 shows the microscopic structures of the spherical NQ formulation. A narrow size distribution was observed for the NQ groups, indicating the presence of a quite homogeneous particle population. The polydispersity index also exhibited a low value of 0.34, as determined by laser scattering. These results demonstrate good agreement between the laser scattering method and TEM.

In vitro drug release study

To examine the performance of the nanodroplets loaded with quercetin, an in vitro drug release test was performed. The in vitro release profiles of quercetin alone and NQ are presented in Figure 3. Release of quercetin from PEG 400 with 20% ethanol was used as the control. As shown in Figure 3, free quercetin in solution showed the highest release, and the NQ formulation showed suppressed and sustained release of quercetin compared with the control group.

Furthermore, to evaluate the release profile after injection, plasma was added to the donor phase and mixed with the test substances to simulate in vivo conditions. The amount of quercetin released from the NQ formulation (in the absence of plasma) showed no significant difference ($P>0.05$) in comparison with NQ mixed with plasma (Figures 3 and 4). To investigate the influence of this novel

Table 1 Characterization of nanodroplets without drug loading and the nanodroplet-encapsulated quercetin formulation by particle size, zeta potential, polydispersity index, and drug encapsulation

	Size (nm)	Zeta potential (mV)	PDI	Encapsulation (%)
Nanodroplets (no drug)	270.1 ± 24.01	-42.18 ± 7.64	0.21 ± 0.01	
NQ	278.6 ± 10.18	-34.66 ± 2.18	0.34 ± 0.01	99.41 ± 0.20

Note: The data are expressed as the mean \pm standard deviation ($n=3$).

Abbreviations: NQ, nanodroplet-encapsulated quercetin; PDI, polydispersity index.

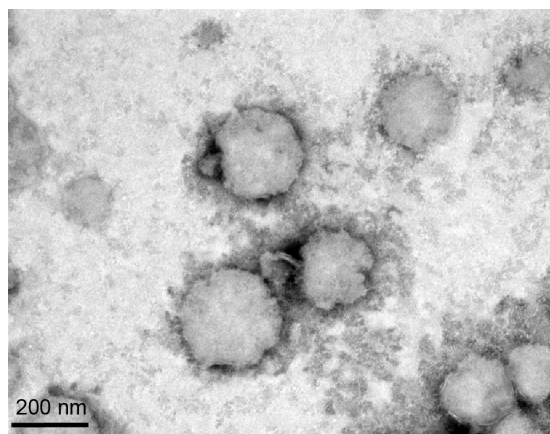


Figure 2 Transmission electron microscopic micrograph of the nanodroplet-encapsulated quercetin formulation. Original magnification 60,000 \times .

use of ultrasound on drug delivery, the amount of quercetin released under ultrasound treatment was examined. Figure 4 shows that ultrasound treatment of 1 MHz (1 minute) produced an increase in drug release from the NQ formulation ($P < 0.05$). The percentage of drug released after 24 hours from the NQ formulation with insonation showed a 2.19-fold and 9.07-fold increase in comparison with the nonultrasound group in the absence and presence of plasma, respectively.

In vivo ultrasonic imaging

To investigate the potential use of nanodroplets for diagnostic application, ultrasonic imaging was used to monitor the appearance of particles in topical (bladder) tissue and the vasculature in rats. No significant difference in

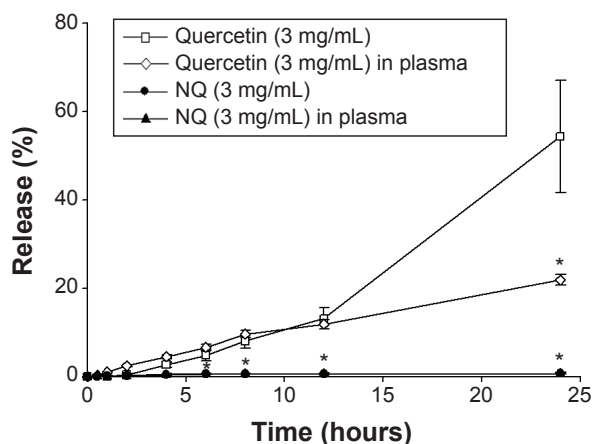


Figure 3 In vitro release profiles for quercetin over time across a cellulose membrane for a control solution of PEG 400 +20% ethanol and perfluorocarbon nanodroplets. A 0.5 mL plasma aliquot was added to the donor compartment of a Franz diffusion cell. Each value represents the mean \pm standard deviation ($n=3$). * $P < 0.05$ versus the quercetin group.

Abbreviations: NQ, nanodroplet-encapsulated quercetin; PEG, polyethylene glycol.

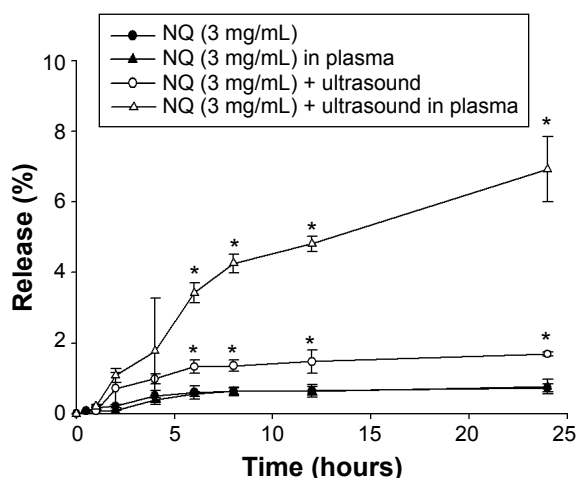


Figure 4 Effect of ultrasound at 1 MHz with an intensity of 2.0 W/cm² and a duty cycle of 20% on in vitro release of quercetin from perfluorocarbon nanodroplets across a cellulose membrane. A 0.5 mL plasma aliquot was added to the donor compartment of the Franz diffusion cell. Each value represents the mean \pm standard deviation ($n=3$). * $P < 0.05$ versus the value for the NQ sample.

Abbreviation: NQ, nanodroplet-encapsulated quercetin.

the ultrasonographic images was observed between the preinjection time point and injection of double-distilled H₂O, but many bubbles appeared in the bladder tissue after injection of the NQ formulation (Figure 5). The boiling point of perfluoropentane is 28.5°C. The increase in the temperature-induced droplet-to-bubble conversion is impeded by the high Laplace pressure inside the nanodroplets. However, nanodroplets are easily converted into bubbles under ultrasonication.^{42–44} The in vivo ultrasonic imaging data provided additional confirmation of droplet-to-bubble conversion.

Figure 6 illustrates the effect of ultrasound-targeted nanodroplets. Figure 6A represents the abdominal vein before NQ injection, which was a blank area. For NQ administration, the femoral vein was catheterized with polyethylene tubing for intravenous administration under anesthesia. Figure 6B shows that some bubbles appeared in the abdominal vein 30 seconds after intravenous administration of nanodroplets via the femoral vein. Ideally, the NQ formulation should be applied for site-specific delivery to areas where selective enhancement of activity by ultrasound is required.⁴⁵ For the next step, to assess the ability of ultrasound-controlled targeted drug delivery, ultrasound-triggered drug-loaded nanodroplets were used. Figure 6C demonstrates that the NQ could be readily directed to specific sites for ultrasonic treatment. After ultrasound triggering, the number of bubbles appeared to decrease, which was confirmed in Figure 6D. These results suggest that the NQ formulation could potentially be used for clinical application to simultaneously enable ultrasound diagnostic imaging and drug targeted delivery.

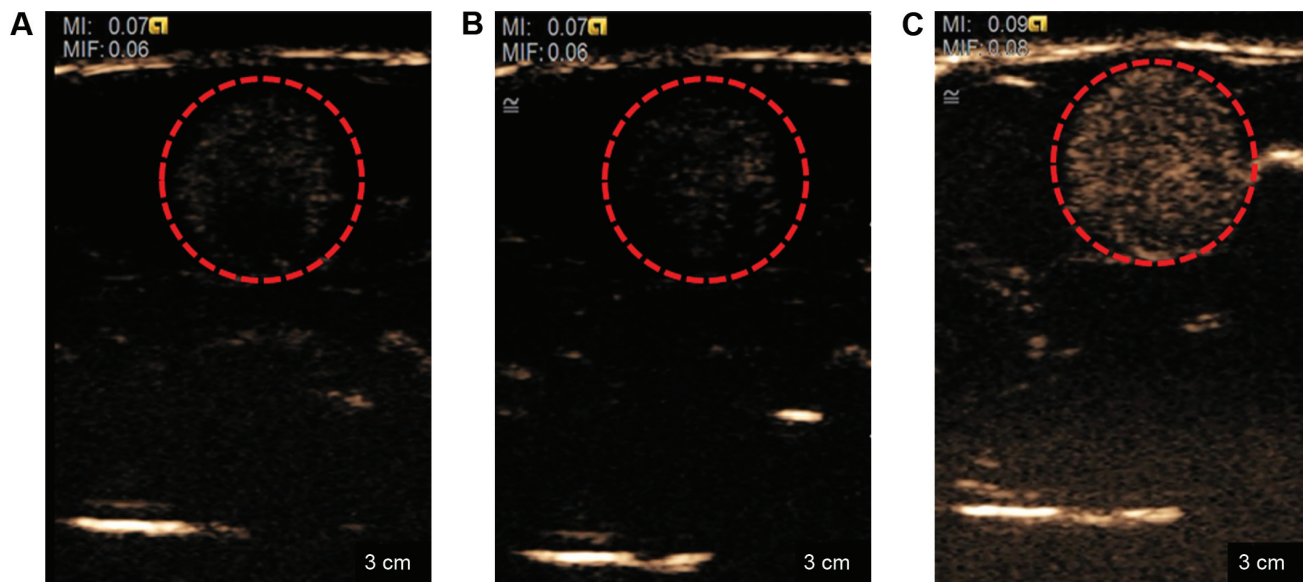


Figure 5 Ultrasonograph of the bladder in the normal rats.

Notes: (A) Preinjection, (B) injection of double-distilled H₂O, and (C) injection of nanodroplets. Red-circled areas indicate monitoring region.

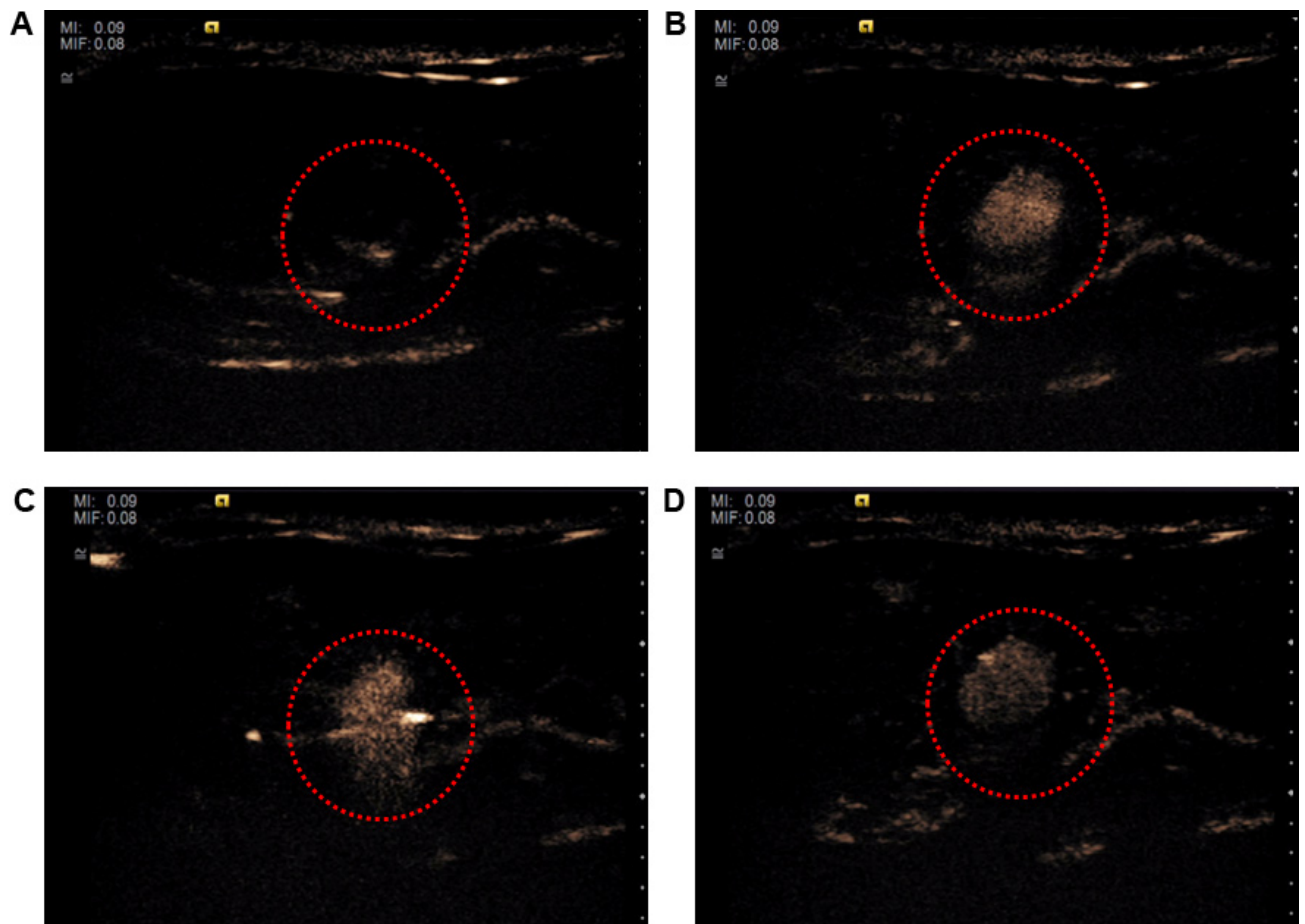


Figure 6 Ultrasonograph of nanodroplets inside the abdominal vein in a rat model.

Notes: (A) Before and (B) after intravenous administration of nanodroplets at 30 seconds. (C) nanobubbles triggered by ultrasonic treatment and (D) after triggering of nanobubbles. Red-circled areas indicate monitoring region.

Pharmacokinetics

To investigate the effects of ultrasound and nanodroplets with regard to the pharmacokinetics of quercetin, the portal vein was used as a topical target for ultrasonic treatment. Four parallel experimental groups were evaluated, ie, quercetin alone, quercetin triggered with ultrasound (quercetin + U), NQ, and NQ triggered with ultrasound (NQ + U). The quercetin concentration-time curves after intravenous administration in the four groups are shown in Figure 7. Quercetin could be detected in plasma up to 45 minutes after administration (3 mg/kg, intravenously), while this time was prolonged to 120 minutes for the NQ groups. The pharmacokinetic parameters were calculated using WinNonlin software version 1.1, and the comparative pharmacokinetic parameters for the four groups are reported in Table 2.

Figure 7 demonstrates that the quercetin concentration-time curves for the free drug and NQ were not significantly affected by ultrasonic treatment. The initial serum concentration ($C_{5 \text{ min}}$) was significantly lower ($P < 0.05$) for the quercetin group than for the nanodroplet formulations (NQ and NQ + U) following intravenous administration.

Table 2 shows a significant increase ($P < 0.05$) in the area under the concentration-time curve (AUC) for the NQ and NQ + U groups ($60.5 \pm 5.9 \mu\text{g/mL per minute}$ and $67.6 \pm 6.8 \mu\text{g/mL per minute}$, respectively) compared with the quercetin alone group ($18.4 \pm 7.0 \mu\text{g/mL per minute}$). These results indicate that the absorption of quercetin increased when the drug was encapsulated in the formulation, regardless of

whether NQ was combined with ultrasonic treatment. These data suggest that the quercetin group was rapidly eliminated from the plasma, whereas the nanodroplet formulations were able to significantly improve the pharmacokinetics of the drug by increasing the AUC, elimination half-life, and $C_{5 \text{ min}}$, and by reducing ($P < 0.05$) clearance.

Discussion

Physical and chemical properties, such as particle size and zeta potential, can affect the pharmacokinetic profile and ultrasonic imaging of nanodroplets.^{11,46} First, we designed and modified quercetin-loaded nanodroplets, which included an evaluation of factors such as dosage, encapsulation, and pharmacokinetic profile. For the conventional mode of injection, the typical injection volume is 1 mL/kg, with a dosage of 1 mg/kg, 3 mg/kg, 5 mg/kg, or 10 mg/kg. We therefore selected 1 mg/mL, 3 mg/mL, and 5 mg/mL quercetin loaded in nanodroplets to assess the feasibility of our experiments. The results showed that 1 mg/kg (1 mg/mL, injection volume 1 mL/kg) of quercetin could not be detected. We ultimately decided that quercetin 3 mg/mL loaded into nanodroplets was suitable for our in vitro and vivo studies.

As shown in Table 1, the particle sizes of the nanodroplets and the NQ formulation were approximately 280 nm, with a low polydispersity index. Small size is an important characteristic for nanodroplets and increases the efficacy of intravenous administration. For example, Ferrara et al reported that the resonance frequency is strongly dependent

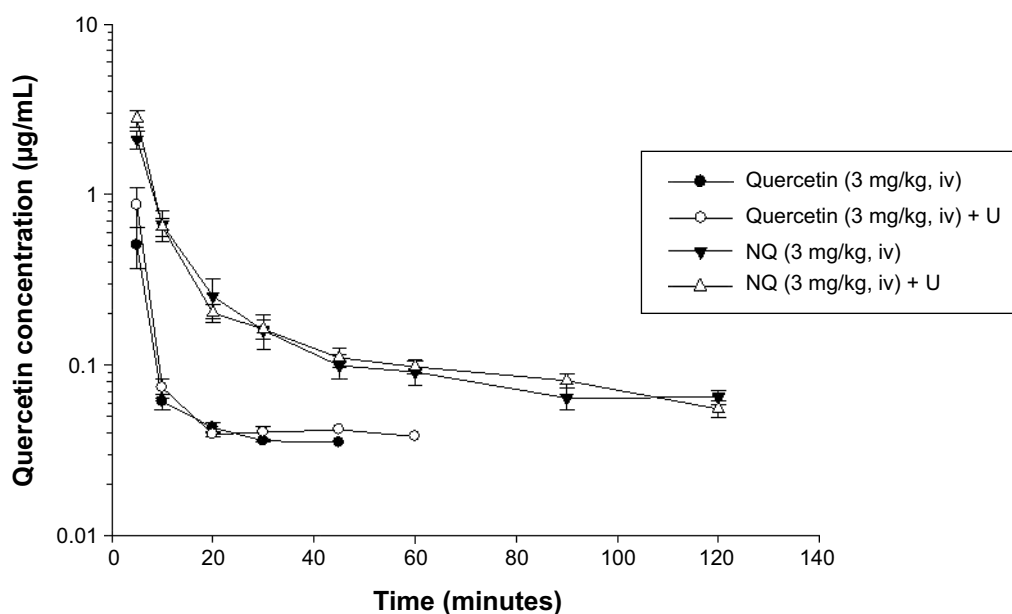


Figure 7 Concentration curve of quercetin in rat plasma after intravenous administration of quercetin 3 mg/kg, quercetin triggered with ultrasound at 3 minutes (quercetin + U, 3 mg/kg), NQ 3 mg/kg, and NQ triggered with ultrasound (NQ + U, 3 mg/kg) at 3 minutes, respectively (mean \pm standard error of the mean; $n=6$).
Abbreviations: iv, intravenously; U, treatment with ultrasound; NQ, nanodroplet-encapsulated quercetin.

Table 2 Pharmacokinetic parameters of quercetin 3 mg/kg and the equivalent quercetin dose for the nanodroplet-encapsulated quercetin formulation in rat plasma after administration of an intravenous bolus

Pharmacokinetic parameters	Quercetin	Quercetin + U (3 min)	NQ	NQ + U (3 min)
C _{5 min} (µg/mL)	0.5±0.1	0.9±0.2	2.3±0.3*	2.8±0.3*
AUC (µg/mL per minute)	18.4±7.0	37.0±10.5	60.5±5.9*	67.6±6.8*
Elimination half-life (minutes)	32±19	29±18	135±43*	72±10*
Clearance (mL/minute per kg)	281±81	183±96	51.6±4.2*	46.1±3.5*

Notes: The data are expressed as the mean ± standard error of the mean (n=6). *P<0.05 versus the quercetin group. C_{5 min} is 5-minute serum concentration after quercetin administration; Quercetin + U (3 min) is ultrasound treatment after 3 minutes quercetin administration; NQ + U (3 min) is ultrasound treatment after 3 minutes NQ administration.

Abbreviations: AUC, area under the concentration–time curve; U, treatment with ultrasound; NQ, nanodroplet-encapsulated quercetin.

on the diameter of the formulation, and specific ultrasound frequencies require a narrow size distribution.²¹ Quercetin is a lipophilic molecule (logP 2.16), and may be encapsulated in a matrix of nanodroplets; however, the structure of quercetin contains many OH groups, so may also be encapsulated within the surface of the shell. As shown in Table 1, the zeta potential decreased from -42.18 ± 7.64 mV to -34.66 ± 2.18 mV when quercetin was loaded into nanodroplets. In theory, quercetin was neutral in the NQ formulation (the pKa of quercetin was 6.44, and the pH value of NQ was 5.5); therefore, some quercetin molecules interacting with the surface of NQ may shield some negative charges, resulting in reduced surface charges being present on NQ.^{34,47}

The uniformity of the particles was confirmed based on the polydispersity index. Our results show that the particle formulations were quite homogeneous (polydispersity index <0.35), and TEM showed that the NQ groups had a narrow size distribution. Previous studies also used similar materials (coconut oil, perfluoropentane, and cholesterol) to produce nanodroplets, and the physical and chemical properties of the nanodroplets are consistent with our data.^{20,36} The suitability of a formulation for clinical application depends on several conditions, and the development of formulations capable of efficiently carrying a payload is one of the most important goals of research.⁴⁸ Our data demonstrate that the NQ formulation achieved a near complete encapsulation efficiency of 99%. The small size and high encapsulation efficiency of this formulation may have a positive effect with regard to pharmacokinetic information.

The morphological characterization of NQ was done using SEM. However, NQ may have undergone structural degradation during preparation of samples for SEM, so disintegration was observed in the images of the NQ formulation. Atomic force microscopy was also used to assess the appearance of NQ, but the apparent dimensions of the NQ were altered during preparation of the sample for processing by atomic force microscopy.⁴⁹ Therefore, we used TEM to

confirm the morphology of NQ. We optimized the method used for TEM sample preparation, including the dye concentration, formulation concentration, and dye settling time, and obtained a clean TEM image (Figure 2).

Release of NQ was preliminarily evaluated in the in vitro study under different conditions and including various factors that may affect the release profiles in this model. The in vitro release rate of quercetin over 24 hours from the control solution of PEG 400+20% ethanol was rapid but could not achieve complete release. This limited amount released may be due to use of an in vitro Franz cell. Because the drug is released into the restricted space of the receptor chamber (5.5 mL) and because of the diffusion area is small (0.785 cm²), the amount of the drug that can be loaded into the receptor compartment is limited, so the concentration gradient between the donor and receptor may have been lost. Nevertheless, this experimental design is still useful for assessing drug release capabilities under different conditions.⁵⁰ An incorporated drug appears to be released in a sustained manner, which is an important characteristic that is often correlated with improved pharmacokinetics and efficacy.⁵¹ Our results indicate that quercetin loaded into nanodroplets was released more slowly than free quercetin, suggesting that release of quercetin can be effectively controlled by use of nanodroplets.

Plasma is a viscous fluid composed of approximately 91% water and 9% other substances, such as proteins, ions, nutrients, and waste products. In this study, plasma was added to the formulation of the NQ to mimic actual in vivo conditions for the release test with ultrasonic treatment. According to the release profiles in the presence of plasma, drug release might be decreased due to increased viscosity and path lengths for drug diffusion.³⁶ Another explanation may be that quercetin binds strongly to albumin and other proteins in plasma.⁵² Previously, ultrasound has been used as an external trigger to induce drug release from drug-loaded carriers. When treated with ultrasound pressure waves,

bubble formulations start to break down and provide a surge in drug release.⁵³ An increase in the amount of quercetin released after ultrasound exposure was observed for the NQ group. When quercetin was encapsulated in nanodroplets, a change in the amount of quercetin released was observed after ultrasound exposure.

Figure 6 confirms that the nanodroplets have features similar to those of microbubbles and have potential for use as vascular contrast agents. Intravesical chemotherapy is a conventional treatment for nonmuscle-invasive urinary bladder cancer.⁵⁴ However, intravesically administered drugs can be eliminated by voiding, and are unable to target certain areas of the bladder. In such situations, use of drug-loaded nanodroplets with ultrasound-triggered disruption is a promising strategy to increase local drug concentrations at the site of pathology while reducing systemic toxicity. Therefore, the results demonstrate the potential applications of nanodroplets for diagnostic imaging and therapy, including the treatment of bladder cancer and imaging of the vasculature.

Although some studies have explored the pharmacological activity of quercetin metabolites (such as the ability of quercetin-3-*O*- β -glucuronide and quercetin-3-*O*- β -glucoside to prevent the damage to red blood cell membranes done by smoking),⁵⁵ most studies have focused on the substantial pharmaceutical effects of quercetin. In this experiment, we focused on improving the therapeutic effect and applications of quercetin via encapsulation into nanodroplets and ultrasound activation.

To investigate the pharmacokinetics of ultrasound-activated, quercetin-encapsulated nanodroplets, a suitable assay system for preparation of samples needed to be developed and optimized. Several methods for sample preparation, such as protein precipitation and liquid–liquid extraction, have been examined. Background interference was observed in the blank plasma extract generated using protein precipitation, whereas no background was observed with the liquid–liquid extraction process. Therefore, ethyl acetate was selected as the liquid solvent for liquid–liquid extraction.

To assess the effects of formulation used and ultrasonic treatment on the pharmacokinetics of quercetin, the pharmacokinetics of four parallel groups (quercetin, quercetin + U, NQ, and NQ + U) were evaluated. Pharmacokinetic studies must take into account the physical welfare of animal subjects. Previous reports have indicated that repeated blood sampling influences the normal physiological conditions of rats and determination of pharmacokinetic profiles.⁵⁶ Thus, the volume of the blood sample and frequency of sampling must be selected carefully, and consequently the time points of the *in vivo* test can be used as a reference for the *in vitro* test.

The results indicate that nanodroplets could prolong the elimination time to achieve a sustained-release effect, which increased both the AUC and elimination half-life and thus reduced drug clearance. Liposomes are composed of phosphatidylcholine-enriched phospholipids and contain mixed lipid chains with surfactant.⁵⁷ The characteristics of the outer shells of our lipid nanodroplets were similar to those of liposomes. Our data are consistent with previous reports,^{5,58} which also found an increased AUC and elimination half-life, as well as reduced clearance for drug-loaded liposomes compared with free drugs. This finding can be attributed to the protection provided by the lipid membranes and slow drug release from the formulation.⁵⁹

A previous *in vitro* report by Paliwal et al indicated that pretreatment of cells with ultrasound may change the concentration of quercetin in treated cell lines.²⁷ Our *in vivo* experiment demonstrated that the $C_{5\text{ min}}$ increased from $0.5 \pm 0.1 \mu\text{g/mL}$ to $0.9 \pm 0.2 \mu\text{g/mL}$ after treatment with ultrasound (Table 2). This observation suggests that treatment with ultrasound may cause the concentration of analyte to increase over a short period of time and have an acute effect. In recent years, many studies have confirmed the efficacy of ultrasound-triggered destruction of bubble formulations for drug delivery, both *in vitro* and *in vivo*.^{13,60} However, inconsistencies between *in vitro* and *in vivo* tests are not unexpected because pharmacokinetic profiles are affected by many factors, including route of administration, the macroenvironment or microenvironment *in vivo*, and protein binding.

Although no statistically significant difference was observed between the pharmacokinetic parameters of NQ and NQ + U, the initial ($C_{5\text{ min}}$) concentration for NQ + U was slightly higher than that in the NQ group. The elimination half-life of NQ + U was 72 ± 10 minutes, which was between that of the quercetin alone (32 ± 19 minutes) and NQ (135 ± 43 minutes) groups, indicating that destruction of NQ during exposure to ultrasound may have caused some drug to be released from the nanodroplets,^{13,61} which slightly affected the pharmacokinetic profile. However, while ultrasound may induce a transient change in pharmacokinetics, encapsulation of quercetin in nanodroplets significantly altered the pharmacokinetic profile of quercetin.

In summary, the results of the *in vitro* tests provided an initial demonstration of the release capability of NQ in the absence of interfering factors, while the *in vivo* tests enabled a complete evaluation of the pharmacokinetic profile of NQ with ultrasound activation, providing a foundation for future clinical application.

Conclusion

In conclusion, we developed quercetin-loaded, lipid-coated nanodroplets and investigated the efficacy of these particles for ultrasound diagnostic imaging of the bladder and vasculature, and ultrasound-triggered drug delivery in rats. To our knowledge, this is the first study of nanodroplets loaded with quercetin that has evaluated their ultrasound-induced pharmacokinetics and potential bioimaging applications. The in vitro and in vivo tests demonstrated that nanodroplets have potential application in simultaneous ultrasonic imaging and drug delivery, and the results and evaluation process could be useful for future preclinical studies.

Acknowledgments

The authors appreciate the assistance of Anthony Venuti in editing the manuscript for language and grammar. Funding for this study was provided in part by research grants from the National Science Council (NSC102-2311-B-001-MY3) of Taiwan and the Taipei City Hospital, Taipei, Taiwan (TCH 10401-62-004).

Disclosure

The authors report no conflicts of interest in this work.

References

- Farokhzad OC, Langer R. Nanomedicine: developing smarter therapeutic and diagnostic modalities. *Adv Drug Deliv Rev.* 2006;58(14):1456–1459.
- Sanhai WR, Sakamoto JH, Canady R, Ferrari M. Seven challenges for nanomedicine. *Nat Nanotechnol.* 2008;3(5):242–244.
- Pouton CW. Formulation of poorly water-soluble drugs for oral administration: physicochemical and physiological issues and the lipid formulation classification system. *Eur J Pharm Sci.* 2006;29(3–4):278–287.
- Fatouros DG, Karpf DM, Nielsen FS, Mullertz A. Clinical studies with oral lipid based formulations of poorly soluble compounds. *Ther Clin Risk Manag.* 2007;3(4):591–604.
- Aithal BK, Sunil Kumar MR, Rao BN, et al. Evaluation of pharmacokinetic, biodistribution, pharmacodynamic, and toxicity profile of free juglone and its sterically stabilized liposomes. *J Pharm Sci.* 2011;100(8):3517–3528.
- Drummond DC, Meyer O, Hong K, Kirpotin DB, Papahadjopoulos D. Optimizing liposomes for delivery of chemotherapeutic agents to solid tumors. *Pharmacol Rev.* 1999;51(4):691–743.
- Toso C, Vallee JP, Morel P, et al. Clinical magnetic resonance imaging of pancreatic islet grafts after iron nanoparticle labeling. *Am J Transplant.* 2008;8(3):701–706.
- Stockhofe K, Postema JM, Schieferstein H, Ross TL. Radiolabeling of nanoparticles and polymers for PET imaging. *Pharmaceuticals (Basel).* 2014;7(4):392–418.
- Wen CJ, Zhang LW, Al-Suwayeh SA, Yen TC, Fang JY. Theranostic liposomes loaded with quantum dots and apomorphine for brain targeting and bioimaging. *Int J Nanomedicine.* 2012;7:1599–1611.
- Rapoport N, Gao Z, Kennedy A. Multifunctional nanoparticles for combining ultrasonic tumor imaging and targeted chemotherapy. *J Natl Cancer Inst.* 2007;99(14):1095–1106.
- Wang Y, Li X, Zhou Y, Huang P, Xu Y. Preparation of nanobubbles for ultrasound imaging and intracellular drug delivery. *Int J Pharm.* 2010;384(1–2):148–153.
- Gessner R, Dayton PA. Advances in molecular imaging with ultrasound. *Mol Imaging.* 2010;9(3):117–127.
- Tsutsui JM, Xie F, Porter RT. The use of microbubbles to target drug delivery. *Cardiovasc Ultrasound.* 2004;2:23.
- Weller GE, Lu E, Csikari MM, et al. Ultrasound imaging of acute cardiac transplant rejection with microbubbles targeted to intercellular adhesion molecule-1. *Circulation.* 2003;108(2):218–224.
- Yin T, Wang P, Zheng R, et al. Nanobubbles for enhanced ultrasound imaging of tumors. *Int J Nanomedicine.* 2012;7:895–904.
- Nguyen AT, Wrenn SP. Acoustically active liposome-nanobubble complexes for enhanced ultrasonic imaging and ultrasound-triggered drug delivery. *Wiley Interdiscip Rev Nanomed Nanobiotechnol.* 2014;6(3):316–325.
- Perera RH, Solorio L, Wu H, et al. Nanobubble ultrasound contrast agents for enhanced delivery of thermal sensitizer to tumors undergoing radiofrequency ablation. *Pharm Res.* 2014;31(6):1407–1417.
- Li SD, Huang L. Pharmacokinetics and biodistribution of nanoparticles. *Mol Pharm.* 2008;5(4):496–504.
- Krupka TM, Solorio L, Wilson RE, Wu H, Azar N, Exner AA. Formulation and characterization of echogenic lipid-Pluronic nanobubbles. *Mol Pharm.* 2010;7(1):49–59.
- Hwang TL, Lin YK, Chi CH, Huang TH, Fang JY. Development and evaluation of perfluorocarbon nanobubbles for apomorphine delivery. *J Pharm Sci.* 2009;98(10):3735–3747.
- Ferrara KW, Borden MA, Zhang H. Lipid-shelled vehicles: engineering for ultrasound molecular imaging and drug delivery. *Acc Chem Res.* 2009;42(7):881–892.
- Soman NR, Lanza GM, Heuser JM, Schlesinger PH, Wickline SA. Synthesis and characterization of stable fluorocarbon nanostructures as drug delivery vehicles for cytolytic peptides. *Nano Lett.* 2008;8(4):1131–1136.
- Ji G, Yang J, Chen J. Preparation of novel curcumin-loaded multifunctional nanodroplets for combining ultrasonic development and targeted chemotherapy. *Int J Pharm.* 2014;466(1–2):314–320.
- Yang PS, Tung FI, Chen HP, Liu TY, Lin YY. A novel bubble-forming material for preparing hydrophobic-agent-loaded bubbles with therapeutic functionality. *Acta Biomater.* 2014;10(8):3762–3774.
- Kaushik D, O'Fallon K, Clarkson PM, Dunne CP, Conca KR, Michniak-Kohn B. Comparison of quercetin pharmacokinetics following oral supplementation in humans. *J Food Sci.* 2012;77(11):H231–H238.
- Lee SM, Moon J, Chung JH, Cha YJ, Shin MJ. Effect of quercetin-rich onion peel extracts on arterial thrombosis in rats. *Food Chem Toxicol.* 2013;57:99–105.
- Paliwal S, Sundaram J, Mitragotri S. Induction of cancer-specific cytotoxicity towards human prostate and skin cells using quercetin and ultrasound. *Br J Cancer.* 2005;92(3):499–502.
- Reinboth M, Wolfram S, Abraham G, Ungemach FR, Cermak R. Oral bioavailability of quercetin from different quercetin glycosides in dogs. *Br J Nutr.* 2010;104(2):198–203.
- Wang P, Heber D, Henning SM. Quercetin increased the antiproliferative activity of green tea polyphenol (-)-epigallocatechin gallate in prostate cancer cells. *Nutr Cancer.* 2012;64(4):580–587.
- Ghosh A, Ghosh D, Sarkar S, Mandal AK, Thakur Choudhury S, Das N. Anticarcinogenic activity of nanoencapsulated quercetin in combating diethylnitrosamine-induced hepatocarcinoma in rats. *Eur J Cancer Prev.* 2012;21(1):32–41.
- Touitou E, Dayan N, Bergelson L, Godin B, Eliaz M. Ethosomes – novel vesicular carriers for enhanced delivery: characterization and skin penetration properties. *J Control Release.* 2000;65(3):403–418.
- Panchagnula R, Desu H, Jain A, Khandavilli S. Effect of lipid bilayer alteration on transdermal delivery of a high-molecular-weight and lipophilic drug: studies with paclitaxel. *J Pharm Sci.* 2004;93(9):2177–2183.
- Saengkrit N, Saeso S, Srinuanchai W, Phunpee S, Ruktanonchai UR. Influence of curcumin-loaded cationic liposome on anticancer activity for cervical cancer therapy. *Colloids Surf B Biointerfaces.* 2014;114:349–356.

34. Aditya NP, Chimote G, Gunalan K, Banerjee R, Patankar S, Madhusudhan B. Curcuminoids-loaded liposomes in combination with arteether protects against *Plasmodium berghei* infection in mice. *Exp Parasitol*. 2012;131(3):292–299.
35. Wang R, Xiao R, Zeng Z, Xu L, Wang J. Application of poly(ethylene glycol)-distearoylphosphatidylethanolamine (PEG-DSPE) block copolymers and their derivatives as nanomaterials in drug delivery. *Int J Nanomedicine*. 2012;7:4185–4198.
36. Fang JY, Hung CF, Liao MH, Chien CC. A study of the formulation design of acoustically active lipospheres as carriers for drug delivery. *Eur J Pharm Biopharm*. 2007;67(1):67–75.
37. Hung CF, Chen JK, Liao MH, Lo HM, Fang JY. Development and evaluation of emulsion-liposome blends for resveratrol delivery. *J Nanosci Nanotechnol*. 2006;6(9–10):2950–2958.
38. Kandadai MA, Mohan P, Lin G, Butterfield A, Skliar M, Magda JJ. Comparison of surfactants used to prepare aqueous perfluoropentane emulsions for pharmaceutical applications. *Langmuir*. 2010;26(7):4655–4660.
39. Tseng L, Liang H, Chung T, Huang Y, Liu D. Liposomes incorporated with cholesterol for drug release triggered by magnetic field. *J Med Biol Eng*. 2007;27(1):29.
40. Hernot S, Klibanov AL. Microbubbles in ultrasound-triggered drug and gene delivery. *Adv Drug Deliv Rev*. 2008;60(10):1153–1166.
41. Sboros V, Glynos E, Pye SD, et al. Nanomechanical probing of microbubbles using the atomic force microscope. *Ultrasonics*. 2007;46(4):349–354.
42. Rapoport NY, Efron AL, Christensen DA, Kennedy AM, Nam KH. Microbubble generation in phase-shift nanoemulsions used as anticancer drug carriers. *Bubble Sci Eng Technol*. 2009;1(1–2):31–39.
43. Rapoport NY, Kennedy AM, Shea JE, Scaife CL, Nam KH. Controlled and targeted tumor chemotherapy by ultrasound-activated nanoemulsions/microbubbles. *J Control Release*. 2009;138(3):268–276.
44. Rapoport N, Nam KH, Gupta R, et al. Ultrasound-mediated tumor imaging and nanotherapy using drug loaded, block copolymer stabilized perfluorocarbon nanoemulsions. *J Control Release*. 2011;153(1):4–15.
45. Klibanov AL. Targeted delivery of gas-filled microspheres, contrast agents for ultrasound imaging. *Adv Drug Deliv Rev*. 1999;37(1–3):139–157.
46. Tsai YM, Chien CF, Lin LC, Tsai TH. Curcumin and its nanoformulation: the kinetics of tissue distribution and blood–brain barrier penetration. *Int J Pharm*. 2011;416(1):331–338.
47. Hwang TL, Aljuffali IA, Lin CF, Chang YT, Fang JY. Cationic additives in nanosystems activate cytotoxicity and inflammatory response of human neutrophils: lipid nanoparticles versus polymeric nanoparticles. *Int J Nanomedicine*. 2015;10:371–385.
48. Liu Y, Miyoshi H, Nakamura M. Encapsulated ultrasound microbubbles: therapeutic application in drug/gene delivery. *J Control Release*. 2006;114(1):89–99.
49. Walczyk W, Schon PM, Schonherr H. The effect of PeakForce tapping mode AFM imaging on the apparent shape of surface nanobubbles. *J Phys Condens Matter*. 2013;25(18):184005.
50. Fang YP, Wu PC, Huang YB, et al. Modification of polyethylene glycol onto solid lipid nanoparticles encapsulating a novel chemotherapeutic agent (PK-L4) to enhance solubility for injection delivery. *Int J Nanomedicine*. 2012;7:4995–5005.
51. Constantinides PP, Lambert KJ, Tustian AK, et al. Formulation development and antitumor activity of a filter-sterilizable emulsion of paclitaxel. *Pharm Res*. 2000;17(2):175–182.
52. Boulton DW, Walle UK, Walle T. Extensive binding of the bioflavonoid quercetin to human plasma proteins. *J Pharm Pharmacol*. 1998;50(2):243–249.
53. Lentacker I, Geers B, Demeester J, De Smedt SC, Sanders NN. Design and evaluation of doxorubicin-containing microbubbles for ultrasound-triggered doxorubicin delivery: cytotoxicity and mechanisms involved. *Mol Ther*. 2010;18(1):101–108.
54. Witjes JA, Hendricksen K. Intravesical pharmacotherapy for non-muscle-invasive bladder cancer: a critical analysis of currently available drugs, treatment schedules, and long-term results. *Eur Urol*. 2008;53(1):45–52.
55. Nadia Salem Alrawaiq AA. Review of flavonoid quercetin: metabolism, bioactivity and antioxidant properties. *International Journal of Pharm Tech Research*. 2014;6(3).
56. Van Herck H, Baumans V, Brandt CJ, et al. Blood sampling from the retro-orbital plexus, the saphenous vein and the tail vein in rats: comparative effects on selected behavioural and blood variables. *Lab Anim*. 2001;35(2):131–139.
57. Fricker G, Kromp T, Wendel A, et al. Phospholipids and lipid-based formulations in oral drug delivery. *Pharm Res*. 2010;27(8):1469–1486.
58. Lee WC, Chang CH, Huang CM, et al. Correlation between radioactivity and chemotherapeutics of the (111) In-VNB-liposome in pharmacokinetics and biodistribution in rats. *Int J Nanomedicine*. 2012;7:683–692.
59. Wei Y, Xue Z, Ye Y, Wang P, Huang Y, Zhao L. Pharmacokinetic and tissue distribution of paclitaxel in rabbits assayed by LC-UV after intravenous administration of its novel liposomal formulation. *Biomed Chromatogr*. 2014;28(2):204–212.
60. Kopeček JA, Haworth KJ, Radhakrishnan K, et al. The impact of bubbles on measurement of drug release from echogenic liposomes. *Ultrason Sonochem*. 2013;20(4):1121–1130.
61. Kiessling F, Fokong S, Koczera P, Lederle W, Lammers T. Ultrasound microbubbles for molecular diagnosis, therapy, and theranostics. *J Nucl Med*. 2012;53(3):345–348.

International Journal of Nanomedicine

Publish your work in this journal

The International Journal of Nanomedicine is an international, peer-reviewed journal focusing on the application of nanotechnology in diagnostics, therapeutics, and drug delivery systems throughout the biomedical field. This journal is indexed on PubMed Central, MedLine, CAS, SciSearch®, Current Contents®/Clinical Medicine,

Submit your manuscript here: <http://www.dovepress.com/international-journal-of-nanomedicine-journal>

Dovepress

Journal Citation Reports/Science Edition, EMBASE, Scopus and the Elsevier Bibliographic databases. The manuscript management system is completely online and includes a very quick and fair peer-review system, which is all easy to use. Visit <http://www.dovepress.com/testimonials.php> to read real quotes from published authors.